Design and Evaluation of Multi-Band RF Energy Harvesting Circuits and Antennas for WSNs

Luís M. Borges[1], Norberto Barroca[1], Henrique M. Saraiva[1], Jorge Tavares[1], Paulo T. Gouveia[1], Fernando J. Velez[1], Caroline Loss[2] and Rita Salvado[2]
[1] Instituto de Telecomunicações/DEM
[2] Textile and Paper Materials Research Unit
Universidade da Beira Interior
Covilhã, Portugal
{m5212, lborges, d708, m1612, m4788, fjv, d1338, rita.salvado}@ubi.pt

Pedro Pinho[3,4], Ricardo Gonçalves[3,5] and Nuno Borges Carvalho[3,5]
[3] Instituto de Telecomunicações, Aveiro, Portugal
[4] Instituto Superior de Engenharia de Lisboa, Lisboa, Portugal
[5] Universidade de Aveiro, Aveiro, Portugal
ppinho@deetc.isel.pt, rgoncalves@av.it.pt, nbcarvalho@ua.pt

Raúl Chavéz-Santiago and Ilangko Balasingham
Intervention Centre,
Oslo University Hospital
Institute of Clinical Medicine
University of Oslo
Norwegian University of Science and Technology (NTNU)
raul.chavez-santiago@rr-research.no, ilangko@medisin.uio.no

Abstract—**Radio frequency (RF) energy harvesting is an emerging technology that will enable to drive the next generation of wireless sensor networks (WSNs) without the need of using batteries. In this paper, we present RF energy harvesting circuits specifically developed for GSM bands (900/1800) and a wearable dual-band antenna suitable for possible implementation within clothes for body worn applications. Besides, we address the development and experimental characterization of three different prototypes of a five-stage Dickson voltage multiplier (with match impedance circuit) responsible for harvesting the RF energy. Different printed circuit board (PCB) fabrication techniques to produce the prototypes result in different values of conversion efficiency. Therefore, we conclude that if the PCB fabrication is achieved by means of a rigorous control in the photo-positive method and chemical bath procedure applied to the PCB it allows for attaining better values for the conversion efficiency. All three prototypes (1, 2 and 3) can power supply the IRIS sensor node for RF received powers of -4 dBm, -6 dBm and -5 dBm, and conversion efficiencies of 20, 32 and 26%, respectively.**

I. Introduction

Nowadays, electromagnetic radio frequency (RF) energy is being transmitted from billions of radio transmitters around the world, including mobile cell phones, handheld radios, mobile base stations, and television/radio broadcast stations. Therefore, there is a wide spectrum of opportunities for harvesting the RF energy, enabling for the creation of energy self-sustainable wireless sensor networks (WSNs) with no need of dedicated transmitters [1]. In addition, one of the major limitations for the adoption of WSNs is the energy available for power supplying the wireless sensor nodes imposed by the finite battery capacity. Since nodes may be deployed in a hostile environment, replacing batteries is often not feasible.

In order to extend the network lifetime, users must limit the application's duty cycle, or use batteries with higher capacity. Other possibility is to use low-power hardware like a low-power processor and radio, at the expense of lower computational capabilities and lower transmission ranges [2].

RF energy harvesting will allow for recharging batteries or supercapacitors and will have a great impact on the lifetime of WSNs. This poses a significant importance as the network size increases, since, for the typical situation, the replacement of the batteries is not practical.

In an outdoor scenario, ambient RF energy harvesting has the advantage of being available at all the hours of the day and night. A solar harvesting node operating during the night presents a blackout period in which its energy source is not available. In an indoor scenario, ambient RF energy harvesting can be attained by using dedicated transmitters, enabling to provide remote power that is controllable through continuous, scheduled or on demand power transmissions [3]. Therefore, RF energy harvesting offers a unique solution, enabling for the implementation of a battery-free wireless sensing solution for 24 hours.

The creation of new innovative medium access control (MAC) mechanisms also play an important role in the network performance [4], since they will enable the optimization of channel utilization in WSNs whilst optimizing the energy consumption. Moreover, with the arising of biomedical sensors as well as suitable network protocols, a new generation of wireless sensor networks have emerged, the so-called wireless body area networks (WBANs). In the context of WBANs, electromagnetic RF energy harvesting is accomplished by using wearable antennas that allow for power supplying the wireless sensor nodes [5].

This work aims at evaluating the developed circuits by considering a dual-band wearable antenna responsible for harvesting the ambient energy in the context of the PROENERGY-WSN project [6]. Three different RF energy harvesting prototypes (1, 2 and 3) with match impedance (by considering short and open-circuit stubs) have been evaluated by means of simulation as well as experiments. Different printed circuit board (PCB) techniques were employed in the fabrication of each one the prototypes.

The remainder of the paper is organized as follows. Section II describes the efficient dual-band antenna considered for collecting RF energy. Guidelines for the choice of textile materials to be used in future wearable antennas are also briefly presented. Section III presents the design considerations for the dimensioning of a 5-stage Dickson voltage multiplier. Section IV presents the simulation and experimental results for the three

prototypes (with match impedance circuit) of the 5-stage Dickson voltage multiplier followed by the discussion of the results. Finally, conclusions are drawn in Section V.

II. Antenna for RF Energy Harvesting

In the work from [7], the spectrum opportunities for electromagnetic energy harvesting from 350 MHz to 3 GHz have been identified, and are considered to conceive multiband antennas for electromagnetic energy harvesting circuits proposed in this work. The obtained results have shown that the GSM (900/1800) bands are the most promising bands for RF energy harvesting.

A. Dual-band antenna

The dual-band antenna dimensions of the wearable antenna prototype for the GSM (900/1800) bands have already been presented in [7]. It has been developed in the context of the PROENERGY-WSN project [6]. The *Cordura*® fabric type was considered for the dielectric substrate, presenting a permittivity, ε_r, of 1.9, loss tangent, *tan* δ, of 0.0098 and relative height of 0.5 mm. For the conductive sections of the antenna an electrotextile (*Zelt*), with an electric conductivity 1.75×10^5 S/m was used.

The variation of the simulated and measured return loss is presented in Fig. 1 for the aforementioned dual-band antenna.

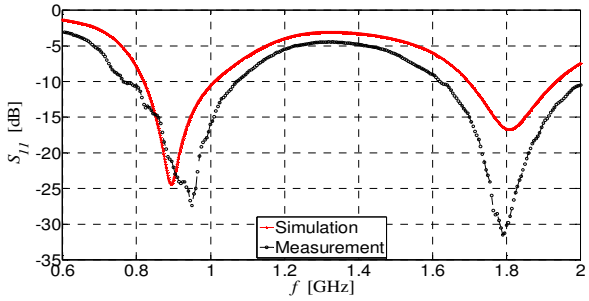

Figure 1. Simulated and measured return loss for the dual-band antenna.

The lowest frequency band considered is from 820-1000 MHz, covering the entire E-GSM band, while the highest considered band is in the range from 1690-1930 MHz, covering the entire DSC1800 band. It is a worth noting, however, that the radiation pattern for the dual-band antenna suffers a deformation at 1800 MHz, as shown in Fig. 1. This is explained by the possible inaccuracy in the cut of the fabrics.

The obtained radiation pattern in the YZ and XZ planes for the proposed antenna is based on numerical simulation with the CST Studio Suite 2011 software and is shown in Fig. 2. The gains for the considered dual-band antenna are about 1.8 dBi and 2.06 dBi, with a radiation efficiency of 82% and 77.6% for the lowest and highest operating frequency bands, respectively.

B. Guidelines to develop wearable flexible antennas

The new generation of garments might contain a wide range of devices and sensors embedded performing a continuous monitoring in various fields, such as health and sport [8], whilst communicating the data to remote receivers.

By considering wearable antennas in the development of energy harvesting devices it allows for binding cloths with communication systems, leading to a more discrete and less intrusive integration of electronic devices.

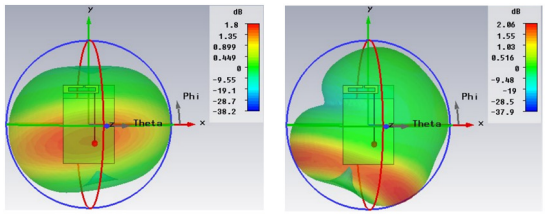

(a) (b)

Figure 2. 3D simulated radiation pattern for the dual-band antenna, including the YZ plane and XZ plane, at a) 900 MHz and b) 1800 MHz.

Specific requirements for wearable antennas are the planar structure and flexible materials. Since textiles, are universally used and easily available, we can assume them as appropriate materials to design wearable antennas. However, a more careful characterization and selection of fabrics is necessary since some characteristics of the materials highly influence the performance of the antenna, e.g., the dielectric constant and the loss tangent, for a specific frequency, the thickness, the moisture content in a specific environment (Regain), as well as the geometrical and mechanical stability of the fabric. Usually, ordinary textiles present a very low dielectric constant, in the range between 1 and 2 (due to the high level of porosity).

Guidelines to develop wearable flexible antennas are addressed in [3] and include the following aspects: A low and stable electrical resistance (≤1Ω/square) of the fabric is desired to minimize losses, where the resistance must be homogeneous over the antenna area, i.e., the variance of the resistance must be low. For the very narrow parts, the cut should be made in the transverse direction of the fabric avoiding the fraying of the yarns [10]. The fabrics for dielectrics should present a low Regain, since textile materials are constantly exchanging water molecules with the environment which might increase their dielectric constant.

III. RF Energy Harvesting Circuits

One of the main aspects that influence RF energy harvesting is the path loss. The Friis free-space equation relates the received power, P_{RF}, at a distance, d, with the transmitted power, P_t, as follows:

$$P_{RF} = P_t \cdot G_t \cdot G_r \cdot \left(\lambda/_{4\pi d}\right)^2 \quad (1)$$

where G_t and G_r are the antenna gains of the transmitter and receiver, respectively. Based on equation (1), we can observe that, the received power depends on the frequency (the higher the frequency is the lower the received power is), and decreases with the square of the distance (path-loss exponent equal to 2). To conceive an RF energy efficient rectifier which enables to rectify and amplify the input voltage (corresponding to P_{RF}), the Cockcroft–Walton and Dickson voltage multiplier circuits can be considered. This work only addresses the Dickson voltage multiplier, as shown in Fig. 3, since, according to [10], both topologies have a similar performance.

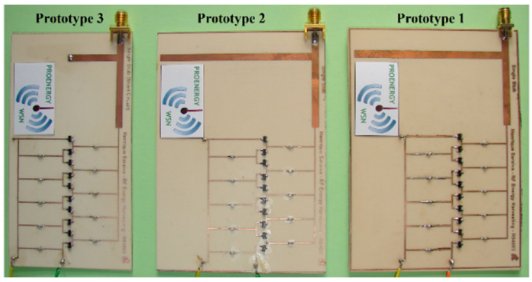

Figure 3. Prototypes of the five stages Dickson voltage multiplier with impedance matching.

In order to evaluate the *N*-stage Dickson voltage multiplier we have used the Advanced Design System (ADS) [11] from Agilent and varied the RF received power, P_{RF}, from -50 dBm to 20 dBm. The considered centre frequency is equal 945 MHz since in [7], the authors have identified the GSM 900 band as the most promising one for RF energy harvesting. The Dickson voltage multiplier (in each one of the prototypes) presented in Fig. 3 is mainly formed by diodes and capacitors in parallel (instead of being in series, as for the Cockcroft–Walton voltage multiplier). Since the input peak voltage from the antenna signal is usually much lower than the diode forward conduction voltage [10], we have considered in the prototypes diodes that present low turn-on voltage. We have chosen the HSMS-2850 Schottky diodes from Avago Technologies optimized for low power applications. In the available literature the number of rectifier stages has a major impact on the output voltage of the Dickson voltage multiplier. According to [12], the output open circuit voltage (OCV) of an *N*-stage Dickson voltage multiplier is given as follows:

$$V_{out} = 2 \cdot N \cdot (V_{in} - V_T) \quad (2)$$

where N is the number of stages, V_{in} is the input voltage amplitude and V_T is the forward conduction voltage of diodes. In equation (2), the output voltage is directly proportional to the number of stages. However, due to practical restrictions (e.g., conversion efficiency) the number of allowable stages is limited. The conversion efficiency, η_0, of a Dickson voltage multiplier is responsible for providing a representation of the overall performance of the circuit, and is defined as the relationship between the output DC power, P_{DC}, and the RF received power, P_{RF}, as follows:

$$\eta_0[\%] = {}^{P_{DC}}/_{P_{RF}} \cdot 100 \quad (3)$$

where the output DC power (P_{DC}) is given by:

$$P_{DC} = V_{DC} \cdot I_{DC} \quad (4)$$

In this work we have chosen the 5-stage Dickson voltage multiplier for RF energy harvesting since according to [13], by adding more stages, the peak of the conversion efficiency curve shifts toward the higher received power region, This is explained by the fact that more than 5 stages will not bring substantial improvement for the power levels considered, due to energy losses along the chain [10]. Moreover, since the wireless sensor nodes need at least 1.8V for operation (i.e., approximately -10 dBm according to [13]), the 5-stage Dickson voltage multiplier is the one which presents the best performance in terms of conversion efficiency. Based on the previous conclusions, the Prototypes 1, 2 and 3 presented in Fig. 3 have been conceived in a PCB fabricated with two layers by using a FR-4 epoxy glass substrate.

IV. Simulation and Experimental Results

In order to evaluate the performance of the 5-stage Dickson voltage multiplier with match impedance, three different prototypes were considered (1, 2 and 3). Prototypes 1 and 2 considers an open-circuit stub, whilst Prototype 3 considers a short-circuit stub as shown in Fig. 3.

Figures 4 and 5 present the output voltage and conversion efficiency for the Dickson voltage multiplier. A load impedance of 100 kΩ is assumed. The simulation results were obtained through a harmonic balanced analysis (i.e., a frequency domain method) that evaluates and assesses the steady state solution of a nonlinear circuit. In Fig. 4 we have considered two levels for the output voltage: the minimum voltage to power supply the sensor node (i.e., 1.8 V) and the advised voltage to power supply the sensor node (i.e., 3 V), which are represented by solid black lines.

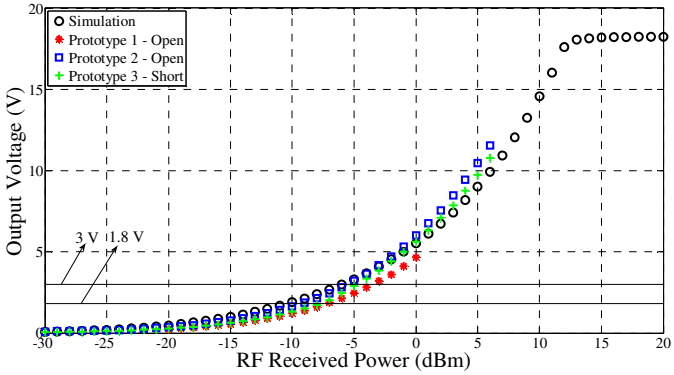

Figure 4. Impact of the RF received power on output voltage for a 5-stage Dickson voltage multiplier with a load impedance of 100 kΩ.

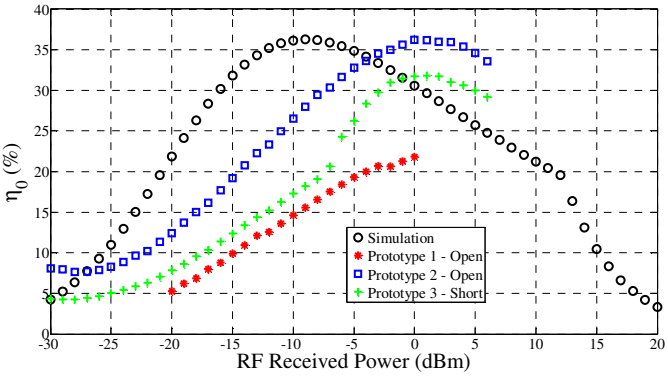

Figure 5. Impact of the RF received power on the conversion efficiency (η_0) for a 5-stage Dickson voltage multiplier with a load impedance of 100 kΩ.

By analysing Fig. 4, we conclude that, by increasing the RF received power, we increase the output voltage. The saturation is theoretically obtained by multiplying the number of stages by the reverse breakdown voltage (i.e., 3.8 V for HSMS-2850 diode). By considering Prototypes 1, 2 and 3 the maximum output voltage obtained experimentally is approximately 4.67, 11.56 and 10.78 V, respectively, which corresponds to RF received powers of 0, 6 and 6 dBm, respectively. In WBAN the nodes equivalent impedance is different for each radio

operation state (RX, TX and SLEEP). According to [13], the value of the impedance from Mica2 in the deep sleep state is 100 kΩ. This value is considered as the impedance reference load for the IRIS motes.

All prototypes include a 5-stage Dickson voltage multiplier along with the match impedance circuit. The development of these prototypes was designed with a match impedance circuit that takes into account the measured impedance from each one of the prototypes as shown in Table I.

TABLE I. MEASURED IMPEDANCE (Z_{IN}) OF PROTOTYPES

Prototype	Z_{in} **(@ 945 MHz)**
1	34.9+j1.66Ω
2	29.6+j19.4Ω
3	51.8+j9.32Ω

Figure 5 presents the effect of the RF received power on the conversion efficiency, η_0. Results show, that Prototype 2 with an open-circuit stub experimentally presents the best results in terms of conversion efficiency. Moreover, by considering and RF received power higher than 0 dBm, Prototypes 2 and 3 outperforms the simulations results in terms of conversion efficiency. Prototype 1 is the one that presents the worst performance in terms of conversion efficiency.

Figure 6 presents the comparison between the simulated and experimental results, for Prototype 2, in terms of the conversion efficiency as a function of the RF received power.

By observing Fig. 6 we conclude that for a load impedance of 100 kΩ, Prototype 2 presents the better results in terms of conversion efficiency. Moreover, by comparing the simulation and experimental results for a load impedance of 100 kΩ, it is observable that a deviation between the simulation and experimental results. This is explained by the fact that the developed prototype presents a mismatching between the antenna and the developed 5-stage Dickson voltage multiplier prototype. The worst case scenario occurs in the case we consider a load impedance of 220 kΩ.

Figure 7 presents the Prototype 3 conversion efficiency as a function of the RF received power in terms of simulation and experimental results for different loads. By analysing Fig. 7 we conclude that for a load impedance of 150 kΩ, Prototype 3 presents better results in terms of conversion efficiency, when the RF received power is lower than -7 dBm. If the RF received power is higher than -7 dBm Prototype 3 attains better results in terms of conversion efficiency by considering a load impedance of 100 kΩ.

In the work from [3], the impact of the load impedance on the conversion efficiency of the 5-stage Dickson voltage multiplier is discussed by analysing its dependence on the RF received power through simulations. Based on the simulation results from [3] the optimal conversion efficiency is achieved when the load impedance is 50 kΩ. If the resistive load value is too low or too high, the conversion efficiency significantly decreases. The deviations between the simulation and experimental results are explained by the PCB manual manufacturing techniques that we employed to develop each one of the prototypes or by not knowing the real parameter values from the diodes in the prototypes. In addition, in the simulations we consider the parameter values supplied by the manufacturer which could induce some error in the simulation results presented. Different PCB fabrication techniques to produce the prototypes also resulted in different values of conversion efficiency.

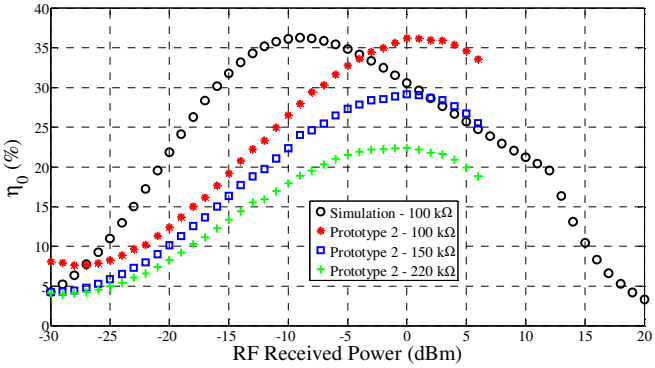

Figure 6. Impact of the RF received power on the conversion efficiency (η_0) for the prototype 2 as a function of the load impedance.

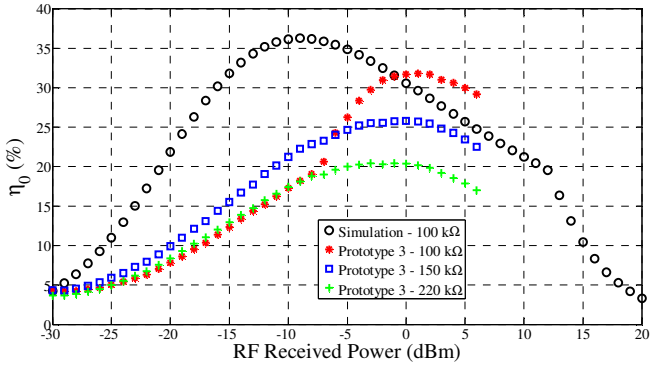

Figure 7. Impact of the RF received power on the conversion efficiency (η_0) for the prototype 3 as a function of the load impedance.

In Prototype 2 and 3 the fabrication was achieved by means of a more rigorous control in the photo-positive method and chemical bath procedure applied to the PCB which resulted in better values for the conversion efficiency. In Prototype 1 the fabrication of the PCB was less rigorous in terms of chemical bath and could have resulted in a more abrasive procedure to the copper film of the PCB. By observing the results obtained it is conclusive that the PCB fabrication allows for attaining better results if the fabrication is controlled in a more rigorous way.

Assuming the abovementioned scenario in which the advised voltage to power supply a IRIS mote is considered, i.e., 3 V, Prototype 1 can power supply the sensor node for a RF received power of -4 dBm, with a conversion efficiency $\eta_0 \approx$ 20%. With Prototype 2 the IRIS mote can be power supplied for a RF received power of -6 dBm, with $\eta_0 \approx 32\%$. Finally, Prototype 3 is capable of supplying an output voltage of 3 V for an RF received power of -5 dBm, with $\eta_0 \approx 26\%$.

Prototype 1 was able to harvest RF energy sufficient to supply a constant voltage of 1.41 V with a load of 100 kΩ whereas in open-circuit it was able to supply with a constant voltage of 2.98 V. These results were obtained by placing Prototype 1 at a distance of 25 meters from the GSM 900 antenna transmitter. The maximum conversion efficiency

(η_{0max}) attained for a load impedance of 100 kΩ is presented in Table II.

TABLE II. MAXIMUM CONVERSION EFFICIENCY

Prototype	η_{0max} (%)
1	22 (@ P_{RF}=0 dBm)
2	36 (@ P_{RF}=0 dBm)
3	32 (@ P_{RF}=1 dBm)

It is observable that Prototype 2 allows for achieving the highest value of conversion efficiency. For the maximum power collected, P_{colmax}, the results obtained are summarized in Table III, whilst considering load impedance of 100 kΩ. Similarly, to the results for the maximum conversion efficiency, the Prototype 2 is the one that allows for achieving the highest value of maximum power collected, but at higher values of RF receiver power, i.e., P_{RF}= 6 dBm.

TABLE III. MAXIMUM POWER COLLECTED

Prototype	P_{colmax} (mW)
1	0.220 (@ P_{RF}=0 dBm)
2	1.33 (@ P_{RF}=6 dBm)
3	1.16 (@ P_{RF}=6 dBm)

Combining the results and the spectral opportunities identified in [3], it is possible that the levels of received power harvested from the environment are not enough to fulfil the goal of power supplying a WBAN. The data collected for the maximum levels of received power are around -27 dBm, which are insufficient to generate an output voltage of 1.8 V. Hence, the development of a super-capacitor storing system that allows for storing little harvested energy (and to use it when the output voltage from the super-capacitor is sufficient to power supply the IRIS mote) is of paramount importance.

V. CONCLUSIONS

In this paper we have presented a wearable dual-band printed antenna, with gains of the order of 1.8-2.06 dBi and 77.6-82% efficiency capable of harvesting electromagnetic energy from the GSM (900/1800) frequency bands.

The design of RF energy harvesting circuits and the choice of textile materials for a wearable antenna have also been analysed. We have also simulated the behaviour of a 5-stage Dickson voltage multiplier for power supplying an IRIS *mote*. Three prototypes (1, 2 and 3) for the 5-stage Dickson voltage multiplier with match impedance were proposed and experimentally characterized. Results show that all three prototypes (1, 2 and 3) can power supply the IRIS sensor node for RF received powers of -4 dBm, -6 dBm and -5 dBm, and conversion efficiencies of 20, 32 and 26%, respectively.

The deviations between the simulation and experimental results for the proposed prototypes are explained by the PCB manual manufacturing techniques that were employed.

ACKNOWLEDGMENT

This work was supported by the Ph.D. FCT grants FRH/BD/66803/2009, SFRH/BD/38356/2007, PhD CAPES grant 9371/13-3, by PEst-OE/EEI/LA0008/2013, PLANOPTI (FP7-PEOPLE-2009-RG), the European Social Fund (ESF), OPPORTUNISTIC-CR, PROENERGY-WSN, INSYSM, CREaTION, EFATraS, COST IC0905 "TERRA", COST IC0902 and COST IC1004.

We would like to thank Prof. Luis M. Correia and Eng. Daniel Sebastião for making the NARDA-SMR spectrum analyser with measuring antenna available to us. The contributions from Mr. Carlos Brito in the production of the printed circuit boards are also much appreciated. We also would like to thank to Eng. Ricardo Freitas from Rhode & Schwarz, for making the signal generator available to us.

REFERENCES

[1] H. Jabbar, Y. S. Song and T. T. Jeong, "RF energy harvesting system and circuits for charging of mobile devices," *IEEE Transactions on Consumer Electronics*, vol. 56, no. 1, pp. 247-253, Feb. 2010.

[2] S. Sudevalayam and P. Kulkarni, "Energy Harvesting Sensor Nodes: Survey and Implications," *IEEE Communications Surveys & Tutorials*, vol. 13, no. 3, pp. 443-461, Sep. 2011.

[3] N. Barroca, H. M. Saraiva, P. T. Gouveia, J. Tavares, L. M. Borges, F. J. Velez, C. Loss, R. Salvado, P. Pinho, R. Gonçalves and N. B. Carvalho, "Antennas and Circuits for Ambient RF Energy Harvesting in Wireless Body Area Net-works," in *Proc. Proc. of the 24th Annual IEEE International Symposium on Personal, Indoor and Mobile Radio Communications (PIMRC'13),* London, United Kingdom, Sept. 2013.

[4] N. Barroca, F. J. Velez and P. Chatzimisios, "Block Acknowledgment Mechanisms for the optimization of channel use in Wireless Sensor Networks", in *Proc. of The 24th Annual IEEE International Symposium on Personal, Indoor and Mobile Radio Communications (PIMRC 2013)*, London, UK, Sep. 2013.

[5] J. S. Bellon, M. Cabedo-Fabres, E. Antonino-Daviu, M. Ferrando-Bataller and F. Penaranda-Foix, "Textile MIMO antenna for Wireless Body Area Networks," in *Proc. of the 5th European Conference on Antennas and Propagation (EUCAP)*, Rome, Italy, Apr. 2011, pp. 428 432.

[6] PROENERGY-WSN, "Prototypes for Efficient Energy Self-sustainable Wireless Sensor Networks," http://www.e-projects.ubi.pt/proenergy-wsn, Apr. 2013.

[7] J. Tavares, N. Barroca, H. M. Saraiva, L. M. Borges, F. J. Velez, C. Loss, R. Salvado, P. Pinho, R. Gonçalves and N. B. Carvalho, "Spectrum Opportunities for Electromagnetic Energy Harvesting from 350 MHz to 3 GHz," in *Proc. of The 7th International Symposium on Medical Information and Communication Technology (ISMICT 2013) - Special Session on Antennas and Propagation for Body Area Network*, Tokyo, Japan, Mar. 2013.

[8] B. Annalisa and D.D.R. Danilo, *Wearable Monitoring Systems*, 1st ed., Springer, New York, USA, 2011.

[9] I. Locher, M. Klemm, T. Kirstein and G. Troster, "Design and Characterization of Purely Textile Patch Antennas," *IEEE Transactions on Advanced Packaging*, vol. 29, no. 4, pp. 777-788, Nov. 2006.

[10] H. Yan, J. G. M. Montero, A. Akhnoukh, L. C. N. de Vreede, and J. N. Burghart, "An integration scheme for RF power harvesting," *in Proc. of The 8th Annual Workshop on Semiconductor Advances for Future Electronics and Sensors*, Veldhoven, Netherlands, Nov. 2005.

[11] Advanced Design System software, http://www.home.agilent.com/en/pc -1297113/advanced-design-system-ads?&cc=PT&lc=eng, Jan. 2013.

[12] U. Karthaus and M. Fischer, "Fully integrated passive UHF RFID transponder IC with 16.7μW minimum RF input power," *IEEE J. Solid State Circuits*, vol. 38, no. 10, pp. 1602-1608, Oct. 2003.

[13] P. Nintanavongsa, U. Muncuk, D. R. Lewis and K. R. Chowdhury, "Design Optimization and Implementation for RF Energy Harvesting Circuits*," IEEE Journal on Emerging and Selected Topics in Circuits and Systems*, vol. 2, no. 1, pp. 24-33, Mar. 201